Article

Cell Reports

Spatiotemporal Control of Forkhead Binding to DNA Regulates the Meiotic Gene Expression Program

Graphical Abstract

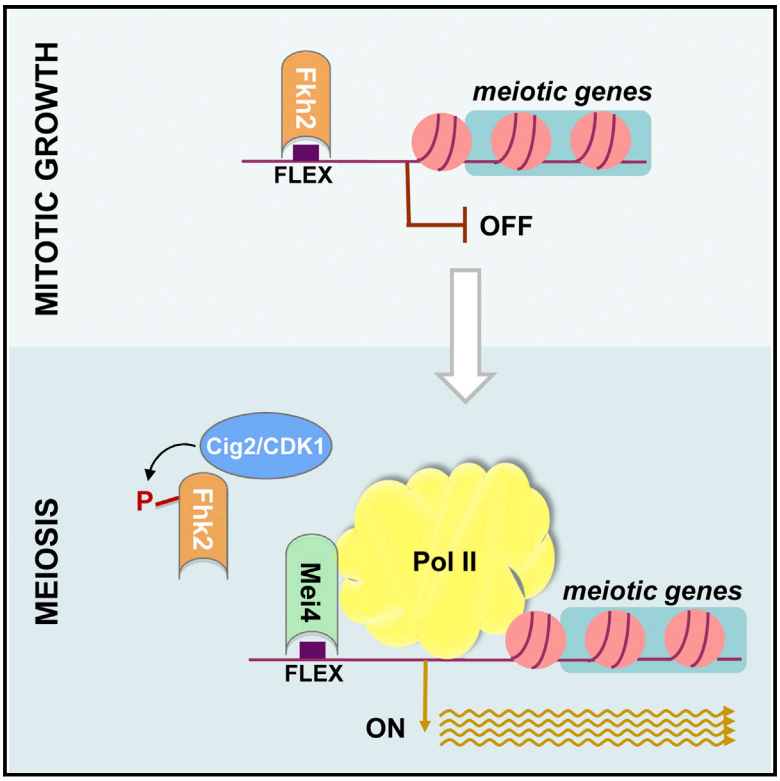

Authors

Isabel Alves-Rodrigues, Pedro G. Ferreira, Alberto Moldón, Ana P. Vivancos, Elena Hidalgo, Roderic Guigó, José Ayté

Correspondence

jose.ayte@upf.edu

In Brief

Alves-Rodrigues et al. show the role of two forkhead transcription factors in the regulation of transcription during meiosis. Although Fkh2 acts as a repressor of transcription preventing the untimely recruitment of Mei4, Fkh2 is also required to maintain an open chromatin structure. This competition is modulated by the phosphorylation of Fkh2 by CDK1 during meiosis.

Highlights

- Mei4 binds a subset of Fkh2-regulated genes only during meiosis
- Fkh2 marks promoters for Mei4 binding during meiosis
- Fkh2 phosphorylation by CDK diminishes its affinity for DNA
- Mei4 and Fkh2 do not coexist on the same promoters

Alves-Rodrigues et al., 2016, Cell Reports *14*, 885–895
February 2, 2016
http://dx.doi.org/10.1016/j.celrep.2015.12.074

Cell Reports
Article

Spatiotemporal Control of Forkhead Binding to DNA Regulates the Meiotic Gene Expression Program

Isabel Alves-Rodrigues,[1] Pedro G. Ferreira,[2,4] Alberto Moldón,[1,5] Ana P. Vivancos,[3] Elena Hidalgo,[1] Roderic Guigó,[1,2] and José Ayté[1,*]
[1]Departament de Ciències Experimentals i de la Salut, Universitat Pompeu Fabra, Barcelona 08003, Spain
[2]Center for Genomic Regulation, Universitat Pompeu Fabra, Barcelona 08003, Spain
[3]Cancer Genomics Group, Vall d'Hebron Institute of Oncology (VHIO), Barcelona 08035, Spain
[4]Present address: Instituto de Investigação e Inovação em Saúde, Universidade do Porto and Institute of Molecular Pathology and Immunology of the University of Porto, Porto 4200-135, Portugal
[5]Present address: Albert Einstein College of Medicine, 1300 Morris Park Avenue, Bronx, NY10461, USA
*Correspondence: jose.ayte@upf.edu
http://dx.doi.org/10.1016/j.celrep.2015.12.074

SUMMARY

Meiosis is a differentiated program of the cell cycle that is characterized by high levels of recombination followed by two nuclear divisions. In fission yeast, the genetic program during meiosis is regulated at multiple levels, including transcription, mRNA stabilization, and splicing. Mei4 is a forkhead transcription factor that controls the expression of mid-meiotic genes. Here, we describe that Fkh2, another forkhead transcription factor that is essential for mitotic cell-cycle progression, also plays a pivotal role in the control of meiosis. Fkh2 binding preexists in most Mei4-dependent genes, inhibiting their expression. During meiosis, Fkh2 is phosphorylated in a CDK/Cig2-dependent manner, decreasing its affinity for DNA, which creates a window of opportunity for Mei4 binding to its target genes. We propose that Fkh2 serves as a placeholder until the later appearance of Mei4 with a higher affinity for DNA that induces the expression of a subset of meiotic genes.

INTRODUCTION

Upon nutrient excess, the fission yeast *Schizosaccharomyces pombe* grows exponentially, replicating its chromosomes and segregating the genetic material into the two identical daughter cells. There are many signals that can perturb a normal cell cycle. Among them, nutrient starvation activates signal transduction pathways that will transiently block cells in G1, initiate conjugation with cells of the opposite mating type, and trigger meiosis (Harigaya and Yamamoto, 2007). At the molecular level, nutrient deprivation induces the expression of several genes, including *mei2*, which encodes an RNA-binding protein that is inactivated during mitotic growth by direct phosphorylation by the protein kinase Pat1 (McLeod and Beach, 1986; Watanabe et al., 1997; Watanabe and Yamamoto, 1994), and *mei3*, which encodes an inhibitor of Pat1 protein kinase (McLeod and Beach, 1988). Pat1 is a master regulator of meiosis, since its inactivation forces cells to enter in meiosis independent of its ploidy. Isolation of *pat1* temperature-sensitive alleles has been an extremely helpful tool that has allowed us to dissect, at the molecular level, the processes that take place through meiosis (Lino and Yamamoto, 1985). More recently, similar results in term of meiotic synchronicity have been achieved using chemical genetics approach where *pat1* alleles can be inhibited with ATP analogs (Cipak et al., 2012; Guerra-Moreno et al., 2012).

With these genetic tricks, it has been possible to prepare highly synchronous cultures of *S. pombe* that undergo pre-meiotic S phase, meiosis I and II, and sporulation. Along many cellular events, it has been shown that meiosis has waves of gene expression along its progression with an ordered cascade of transcription factors that have to be sequentially activated (Mata et al., 2007). Mei4 has a central role in this transcriptional cascade, being a meiosis-specific transcription factor that induces a set of genes that are required for initiation of meiosis I (Horie et al., 1998). Mei4 is also able to promote pre-mRNA splicing of a subcluster of mid-meiosis intron-containing genes (Moldón et al., 2008), where intron retention has been shown to be a safe-lock mechanism that prevents the presence of several gene products that are toxic if produced in non-meiotic cells (Malapeira et al., 2005). The Mmi1 system is another major mechanism that also prevents the toxicity of meiosis-specific genes in mitotic cells (Harigaya et al., 2006). Mmi1 is a YTH-family RNA-binding protein that in mitotic cells recognizes some meiotic mRNAs and sends them to destruction through the exosome (Yamashita et al., 2012).

Mei4 is a transcription factor of the Forkhead/Winged-helix family and binds to FLEX motifs (GTAAA(C/T)A) in promoters of genes that are under its regulation (Horie et al., 1998; Moldón et al., 2008). Fkh2, another forkhead transcription factor, has been implicated in the regulation of the same cluster of meiotic genes (Moldón et al., 2008). However, Fkh2 has a broader relevance on transcription regulation in fission yeast, since it also has a major role in the regulation of cell-cycle-dependent transcription, specifically controlling the M-to-G1 transcriptional wave of the cell cycle (Papadopoulou et al., 2008). While in meiosis Fkh2 works together with Mei4, during vegetative

growth, Fkh2 partners with Sep1, which also contains a forkhead domain (Buck et al., 2004). Interestingly, there is a common theme in these pairs: Fkh2 is always related to repression of gene expression, while Mei4 and Sep1 are directly involved in meiotic and mitotic gene activation, respectively (Moldón et al., 2008; Papadopoulou et al., 2008). Similarly, in budding yeast, forkhead transcription factors are involved in the activation and repression of different subsets of cell-cycle-regulated genes (Darieva et al., 2010; Voth et al., 2007).

Chromatin structure is essential to protect the genome integrity, but at the same time, it acts as a barrier to transcription since it limits DNA accessibility to transcription factors, hindering their target sequences. For a successful interaction of a transcription factor with genomic regulatory elements, local rearrangements of nucleosomes must occur. In this context, pioneer factors are a class of proteins that are able to find and bind their target sequences in chromatin when other transcription factors cannot reach them. Thus, they are sufficient to trigger competency of transcription and it is proposed that they continue to bind DNA prior to the transcriptional activation, opening up local chromatin structure and increasing accessibility of chromatin to other transcription factors (Voss and Hager, 2014). In many instances, pioneer factors promote transcription factor binding to their own DNA recognition motifs. Members of the forkhead box (FOX) family of proteins have been widely implicated as pioneer factors (Lee et al., 2005). Neither Fkh2 functional interaction with Mei4 nor its molecular mechanism as transcription factor is well understood. Here, using chromatin immunoprecipitation sequencing (ChIP-seq), we show that the forkhead transcription factors Fkh2 and Mei4 are loaded into meiotic promoters in a fixed sequential order, where Fkh2 binds first, poising the promoters where Mei4 has to be loaded later during meiosis.

RESULTS

Genome-wide Binding of Fkh2 and Mei4 during Meiosis

In previous work, we reported that Mei4 and Fkh2 work together to regulate the transcription and splicing of a subset of meiotic genes whose expression peaks in meiosis I (Moldón et al., 2008). How these two transcription factors function in the control of meiotic progression is not well understood, although Fkh2 has been linked to repression and Mei4 to the activation of a specific program of splicing during meiosis. To get unbiased knowledge of how these two transcription factors work together, we performed a genome-wide ChIP-seq for Fkh2 and Mei4 in synchronized meiotic cultures (Figure 1A). We successfully mapped 110 million reads to the *S. pombe* genome, selecting uniquely mapped reads for further analysis, detecting Fkh2 binding at 379, 619, and 741 sites during mitotic growth 3 and 4 hr into meiotic progression, respectively, and Mei4 binding at 373 and 100 sites after 3 and 4 hr into meiotic progression, respectively. After discarding all those sites that were located downstream of the annotated transcription start sites (TSSs), we reduced the number of potential binding peaks to ~70% (for Fkh2) or 50% (for Mei4) (Figure 1B; a complete list of genes for each category is shown in Table S1). Although this pattern of binding site utilization is consistent with the role of Fkh2 during mitotic growth, we could only detect a small number of exclusively mitotic peaks (7 out of 227), indicating that those genes that are regulated in an Fkh2-dependent manner during mitotic growth are also under Fkh2 regulation during meiosis. The vast majority of the Mei4 binding peaks (45 out of 48) are also bound by Fkh2 during meiosis, indicating that only a small subset of the Fkh2-regulated genes might also be regulated by Mei4 during meiosis (45 out of 383).

Although it is known that forkhead transcription factors bind FLEX motifs, we also performed de novo motif search to identify specific sequences bound by Fkh2, Mei4, or both (Figure 1C). Notably, we identified highly similar motifs in the three sets of promoters, with the particularity that in the Mei4 peaks (alone or together with Fkh2), the motif was extended toward the 3′ end with a stretch of adenines. This, we believe, could explain the specificity for Mei4 binding. We then analyzed individually the kinetics of each one of the Fkh2 and Mei4 peaks and could manually classify them in three different groups, according to the timing and characteristics of Fkh2 and Mei4 binding (Figure 1D). The first group of genes included mitotic genes, whose expression is known to be regulated by Fkh2 and another transcription factor belonging to the forkhead family, Sep1 (Buck et al., 2004; Papadopoulou et al., 2008); this group of genes include *fkh2*, *plo1* (which encodes Polo-like kinase 1), and *SPBC646.16*, among many others. The main characteristic of this first group of genes is that Mei4 is never present in their promoters, neither during vegetative growth nor during meiosis. The second group of genes, including *mug133*, *mde3*, and *mde2*, shows Fkh2 binding during mitotic growth and Fkh2 and Mei4 binding during meiosis. Finally, the main characteristic of the last group of genes (that includes *mde9*, *mfr1*, and *ppk9*) is the absence of Fkh2 peaks during mitotic growth and binding of both Fkh2 and Mei4 during meiosis. The last two groups of genes contain genes whose transcription is induced during meiosis and whose expression during mitotic growth is minimal or absent (Mata et al., 2002).

To obtain a better knowledge of Mei4 and Fkh2 binding kinetics in the different sets of genes, we analyzed by chromatin immunoprecipitation (ChIP) their binding during a complete meiotic time course (Figures 2A–2E). While there was an undetectable binding of Mei4 to the first group, irrespective of their expression during meiosis (Figures 2A and 2B), we could confirm binding of Mei4 during meiosis in the second and third group of genes (Figures 2C and 2D). Interestingly, we could detect an earlier binding of Mei4 to the genes that had Fkh2 previously bound during mitotic growth (i.e., *mde3* versus *mde9*). In both sets of genes, binding of Mei4 was at least partially dependent on Fkh2, since in a *Δfkh2* strain binding of Mei4 was delayed and diminished (Figures 2C and 2D, right). The effect that Fkh2 has on Mei4 binding to its target promoters is clearly noticeable, since binding of Mei4 was impaired or delayed in all the four genes that were analyzed, without affecting the amount of Mei4 that was detected in the cells (Figure S1). Furthermore, quantification of this global effect showed that in all four genes, Mei4 bound poorly to its target genes in the absence of Fkh2, and this difference had statistical significance, at least for *mfr1*, *mde3*, and *mde2* (Figure 2E). In fact, when taking into account all the genes together, the effect of Fkh2 on Mei4 binding was statistical significant ($p < 0.05$). It is worth mentioning that the effect of the other fission yeast forkheads, Fhl1 and Sep1, was

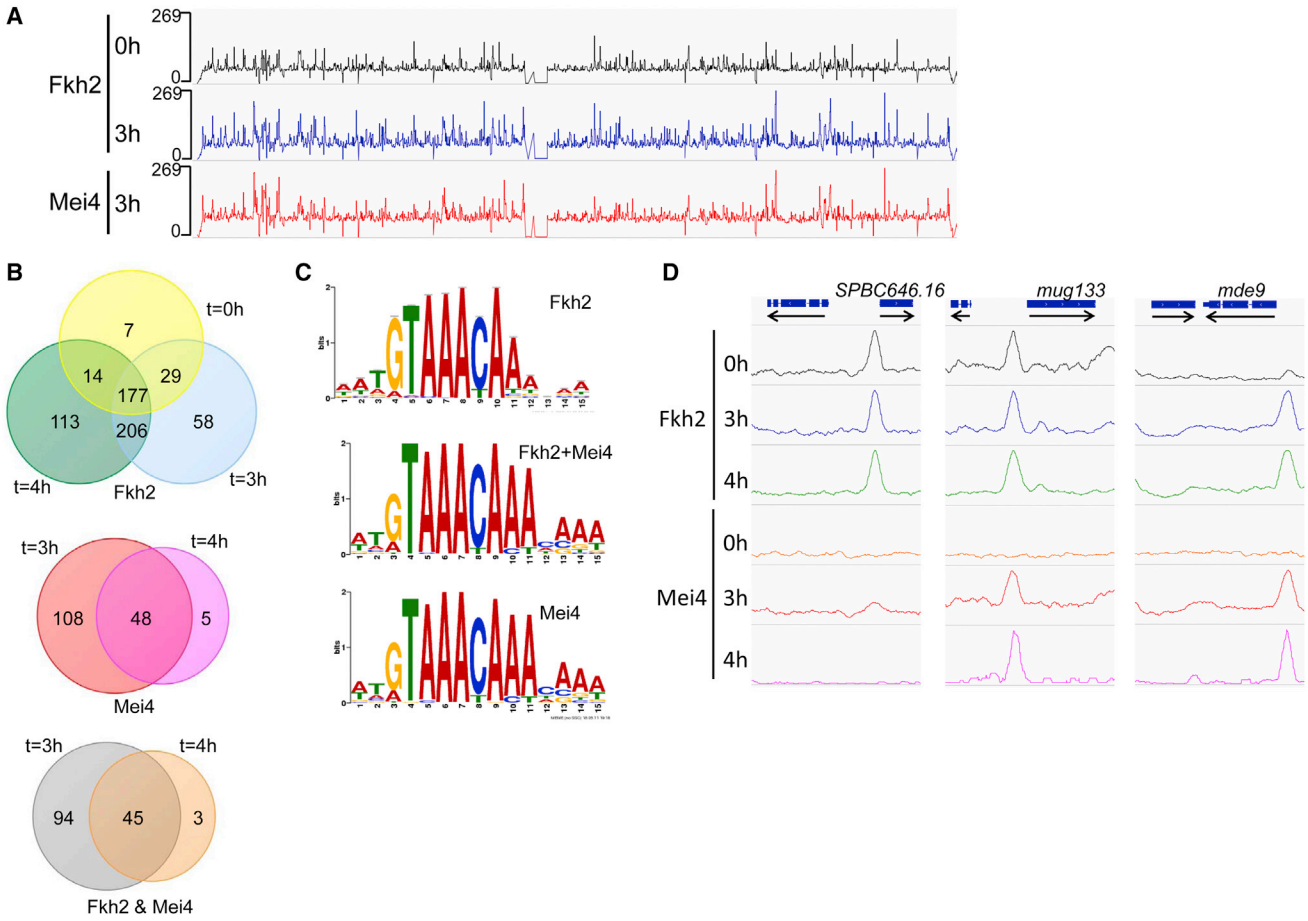

Figure 1. Genome-wide Analysis of Fkh2 and Mei4 Chromatin Binding

(A) Plots show a ChIP-seq genome-browser view of binding of Fkh2 at 0 (black) and 3 (blue) hr and Mei4 at 3 (red) hr into synchronous meiosis along the entire chromosome 3 of *S. pombe*. Number of tags is indicated in the y axis. The region with no information in the middle of the plots corresponds to the centromere.

(B) Venn diagrams showing the overlap between significant peaks for Fkh2 at 0, 3, and 4 hr into meiosis (top), Mei4 at 3 and 4 hr (middle), and common to both proteins (bottom). Numbers indicate the number of binding peaks for each protein. The complete list of genes of each category is shown in Table S1.

(C) De novo motif discovery identifies a similar sequence binding for Fkh2, Mei4, and Fkh2 in co-occurrence with Mei4 (Fkh2 + Mei4) but with an extension toward the 3′ end of the motif when Mei4 is able to bind.

(D) Plots showing the binding profile of Fkh2 and Mei4 representative genes of each class: only Fkh2 binding in mitosis and meiosis (*SPBC646.16*), Fkh2 constitutive binding in mitosis and Mei4 binding in meiosis (*mug133*), and both proteins binding exclusively at mid-meiosis (*mde9*).

shown to be negligible both in transcription and in splicing during meiosis (Moldón et al., 2008). Since we could only detect binding of Sep1 and Fhl1 by ChIP to the mitotic gene *plo1* (which we used as positive control) and barely any binding to the meiotic genes (Figure S2), we can disregard any effect of Sep1 or Fhl1.

The meiotic transcription and splicing program is altered in the absence of either Fkh2 or Mei4 (Moldón et al., 2008). Similarly, during vegetative growth, an *fkh2* mutation has a more profound effect on transcription than a mutation in its mitotic partner, *sep1* (Buck et al., 2004; Papadopoulou et al., 2008). With the exception of few genes corresponding to the *mde9* group, it seems that Fkh2 remains constitutively bound to its target promoters during mitosis and meiosis and is required for the timely loading of Mei4 in meiosis. This is reminiscent of pioneer factors that serve as placeholders for later transcription factors and manage to bind DNA independent of nucleosome and chromatin structure (Xu et al., 2009; Zaret and Carroll, 2011). To test whether Fkh2 is required for chromatin organization of some meiotic genes, we determined the nucleosomal position at *mde9* by nucleosome scanning (Figure 2F). In our hands, nucleosome positions in wild-type cells resemble the one recently described in a genome-wide nucleosomal map (Soriano et al., 2013). Interestingly, the FLEX boxes in *mde9* are situated in nucleosome-depleted regions (NDRs) and in the −2 nucleosome in mitotic cells, but when cells are induced into meiosis, this −2 nucleosome is evicted, enlarging the NDR. This points to the possibility that Fkh2 might be competing with histones to enlarge the NDR. To support this hypothesis, we observed that deletion of *fkh2* has no effect in mitotic cells (since Fkh2 is not loaded onto *mde9* until initiation of the meiotic program; Figure 2C). However, deletion of *fkh2* results in general nucleosome disorganization in the

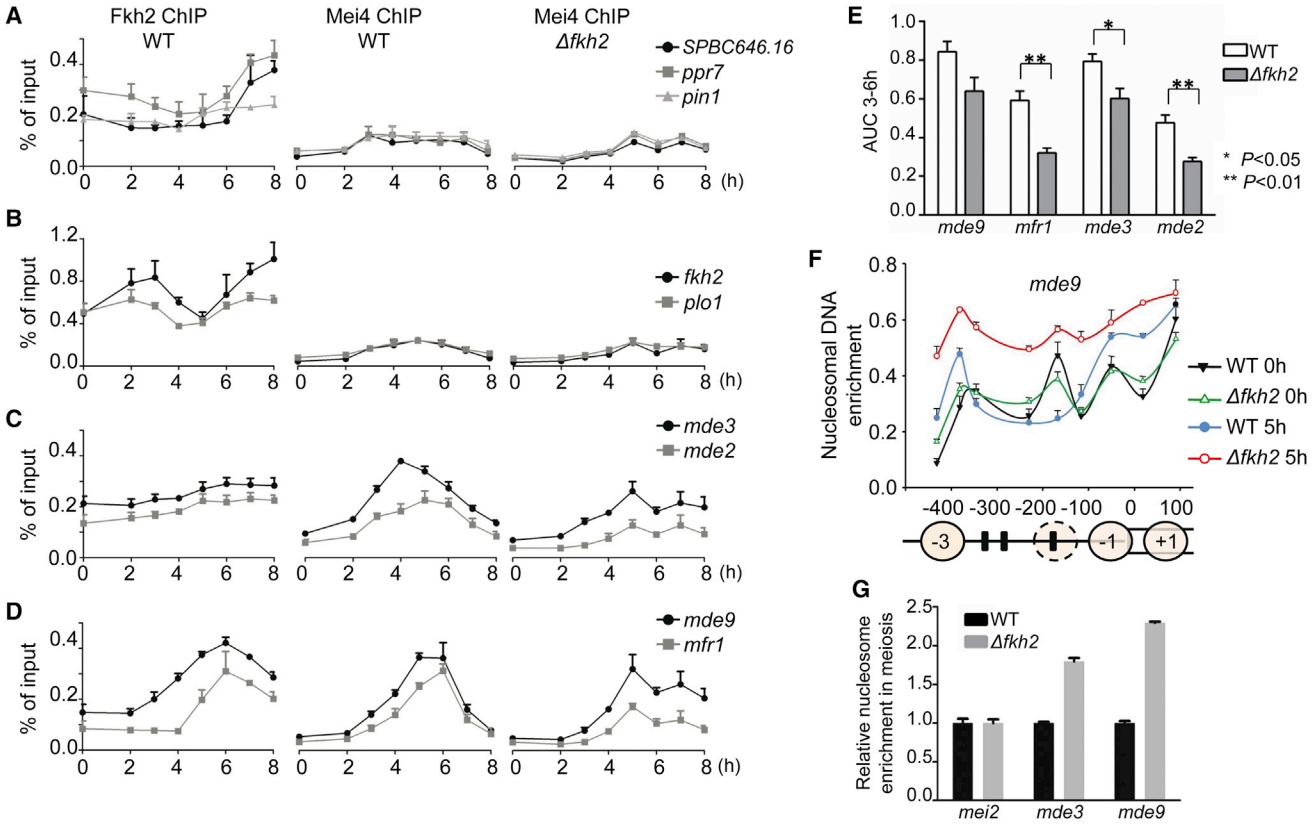

Figure 2. Fkh2 Marks the Timing of Mei4 Loading in Meiosis

(A) Fkh2 and Mei4 ChIP analysis during synchronous meiosis in wild-type (WT) and *Δfkh2* cells. Chromatin was immunoprecipitated with α-HA antibody, and the isolated DNA was used to amplify the promoter region of a subset of genes that are not expressed during meiosis but whose expression in mitosis is regulated by Fkh2. Plots represent the average of at least three different biological replicates ± SEM. Similar synchronicity of meiosis was observed for all the strains.

(B) Same as in (A), but the group of genes analyzed corresponds to genes that are expressed in mitosis and meiosis. Plots represent the average of at least three different biological replicates ± SEM.

(C) Same as in (A), but the group of genes analyzed corresponds to genes that are only expressed in meiosis and show pre-binding of Fkh2 during mitosis. Plots represent the average of at least three different biological replicates ± SEM.

(D) Same as in (A), but the group of genes analyzed corresponds to genes that are only expressed in meiosis and show no binding of Fkh2 during mitosis. Plots represent the average of at least three different biological replicates ± SEM.

(E) Mei4 ChIP analysis during synchronous meiosis in WT and *Δfkh2* cells. The bars represent the area under the curve (AUC) of the graphs represented in Figures 2C and 2D in mid-meiosis (3–6 hr) when Mei4 protein is expressed. Student's t test was used to calculate the statistical significance (*$p < 0.05$ and **$p < 0.01$ between WT and *Δfkh2* cells). Error bars (SEM) were calculated from three independent experiments.

(F) Fkh2 is required for proper nucleosomal organization at *mde9* during mid-meiosis. Mono-nucleosomes were isolated from WT and *Δfkh2* cells in mitotic growth and mid-meiosis. qPCR was performed using primers covering 500 bp flanking the ATG codon. Nucleosomes are represented as circles and numbered relative do the ATG codon, ORFs as open white rectangles, and FLEX motifs as small black rectangles. Error bars (SEM) were calculated from three biological replicates.

(G) Relative nucleosome occupancy was determined as described above using primers for *mei2* (control), *mde3*, and *mde9* promoters during mid-meiosis. The graph shows the nucleosome occupancy at *Δfkh2* cells relative to wild-type strain, with an assigned value of 1 in each gene. Error bars (SEM) were calculated from biological triplicates.

See also Figures S1 and S2.

proximal promoter region of *mde9* once cells enter into meiosis, probably hiding the FLEX boxes inside nucleosomes. Interestingly, we observed a similar effect in *mde3*, where we detected a 2-fold nucleosomal enrichment in meiotic *Δfkh2* cells when compared to meiotic wild-type cells (Figure 2G). As a control, we mapped the nucleosomal positions at *mei2*, a meiotic induced gene that lacks FLEX elements and whose transcription is not regulated by any forkhead transcription factor. Thus, Fkh2 binds its target promoters maintaining an open chromatin structure that facilitates the later loading of Mei4 to a subset of Fkh2-regulated genes.

Phosphorylation of Fkh2 Decreases Its Affinity for DNA

Fkh2 was described to have periodic transcription during the mitotic cell cycle with a peak at M phase (Bulmer et al., 2004; Rustici et al., 2004). The protein level also peaks during M phase, with multiple cell-cycle-specific phosphorylation events. Some of these phosphorylations have been described to have a critical

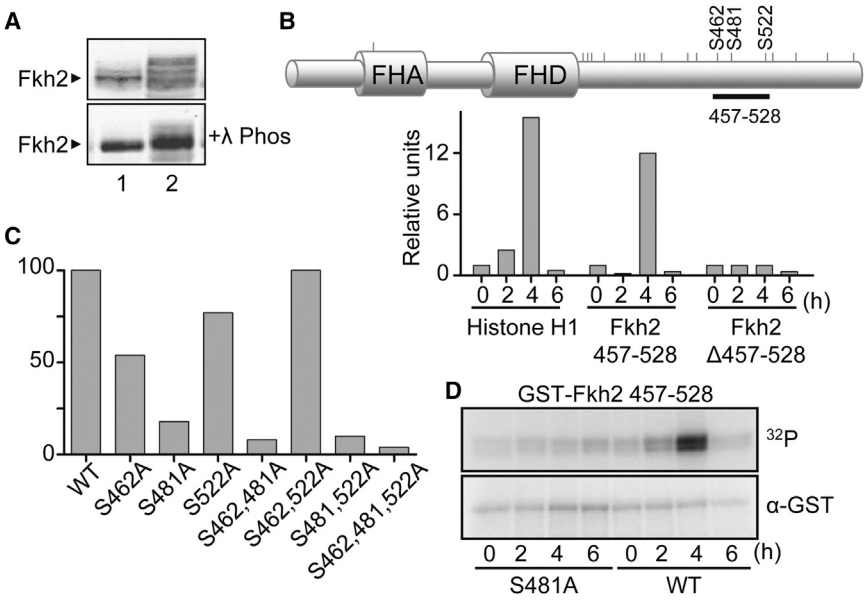

Figure 3. Cig2/CDK1 Phosphorylates Fkh2 during Meiosis

(A) Western blot of Fkh2 during vegetative growth (lane 1) or synchronous meiosis (lane 2). Extracts were prepared from mid-meiosis, separated in an 8% polyacrylamide gel, and treated or not with λ-phosphatase. Western blot detection was performed with α-HA antibodies.

(B) Schematic of Fkh2 primary structure and domains (Forkhead [FHD] and Forkhead Associated [FHA]), with the putative CDK phosphosites indicated as vertical bars. For the in vitro kinase assays, cells expressing Cig2-HA (from the endogenous locus) were harvested at different meiotic time points and Cig2-HA/CDK was immunopurified and used in the kinase assays. Histone H1 (control), Fkh2 Δ457–528, and Fkh2 457–528 were used as substrates of Cig2-HA/CDK, and signal was quantified and plotted relative to the signal at 0 hr.

(C) Quantification of a kinase assay using purified Cig2-HA isolated from synchronous meiotic culture. Substrates used in this assay contained amino acids 457–528 from Fkh2 or the mutant forms indicated at the bottom. The graph is plotted as percentage of the wild-type Fkh2 phosphorylation signal.

(D) Kinase assay using Cig2-HA from a complete meiotic time course, using as substrates either wild-type Fkh2 457–528 (WT) or the Ser481Ala mutant (S481A). α-GST western blot is shown as loading control.

role also during meiosis (Shimada et al., 2008). We have detected that both proteins, Fkh2 and Mei4, peaked around meiosis I (data not shown). Fkh2 displayed noticeably slower mobility in western blots, mainly in mid-meiosis (Figure 3A). When we treated the protein samples with λ phosphatase, all the bands collapsed to the fast migrating form, indicating that the changes in mobility were due to phosphorylation (Figure 3A). The primary structure of Fkh2 revealed 18 putative phosphorylation sites by Cdks ([S/T]-P), none of which were within the forkhead domain and just one of which was within the FHA domain (Figure 3B). We decided to investigate whether Fkh2 is phosphorylated in a CDK-dependent manner. Specifically, we considered the cyclin Cig2, since this is the main cyclin during fission yeast mid-meiosis (Borgne et al., 2002) and because a genetic interaction between Cig2 and Mei4/Fkh2 has been described (Malapeira et al., 2005). We performed in vitro kinase assays using immunoprecipitated Cig2-HA from different time points of meiosis and recombinant GST-Fkh2 protein purified from *Escherichia coli* as substrates. Different truncated versions of Fkh2 were used to delimit the candidate S/T-P sites between amino acids 457 and 528. As shown in Figure 3B, a truncated Fkh2 (457–528) could be specifically phosphorylated by Cig2 at the 4 hr time point of meiosis, while the complementary protein (Fkh2 Δ457–528) was not phosphorylated.

In the delimited region there are only three putative phosphorylation sites: Ser462, Ser481, and Ser522. We analyzed individual, double, and triple specific-site mutants to find the specific substrate residue(s). All mutants carrying Ser481Ala showed a diminished phosphorylation signal (<20% of wild-type signal), whereas the rest retain their ability to be phosphorylated, at least partially (Figure 3C). To confirm this result, we performed a complete time course using extracts from synchronous meiosis in our kinase assays. This experiment allowed us to determine that Ser481 was the main phosphorylation site by Cig2 during meiosis (Figure 3D).

Next, we wanted to understand the consequences of Fkh2 phosphorylation on Ser481. One obvious hypothesis is that phosphorylation could affect Fkh2 DNA-binding affinity. To test this, we first measured the K_D of Fkh2 and Mei4 for the FLEX motifs in the *mde3* and *mde9* promoters using an electrophoretic mobility shift assay (EMSA). As shown in Figures 4A and 4B, both proteins have a similar K_D for the promoters (19.9 nM and 14.29 nM, respectively), which are in the range of the calculated protein concentration in the nucleus of 24 nM and 16 nM, respectively (Carpy et al., 2014). A similar K_D was obtained for the *mde9* promoter. We also measured the K_D of Fkh2 in which Ser481 was replaced by either alanine (which renders an Fkh2 that cannot be phosphorylated by Cig2/Cdk1) or aspartic acid (which mimics a constitutively phosphorylated Fkh2). Interestingly, the phosphomimetic mutant had a 2.8-fold decreased affinity for the FLEX motifs (14.0 nM versus 39.0 nM), pointing to the fact that once phosphorylated at Ser481, Fkh2 might have diminished binding activity toward the target genes, at least when compared to Mei4. To be sure that replacing a small amino acid like serine by a more bulky one like aspartic acid was not disturbing the structure of Fkh2 and thus the decrease on its DNA-binding activity was merely an effect of the loss of the proper structure, we also created mutants in which Ser481 was replaced by asparagine or valine. Both mutants had a K_D for their target promoters that was similar to wild-type Fkh2 (Figure S3), indicating that possibly the negative charge in the residue 481 was responsible for decreasing Fkh2 DNA-binding activity.

To address the possibility that phosphorylation of Fkh2 at Ser481 by Cig2/Cdk1 was directly responsible for its decrease in affinity to DNA, we used either Fkh2 or the S481A mutant as

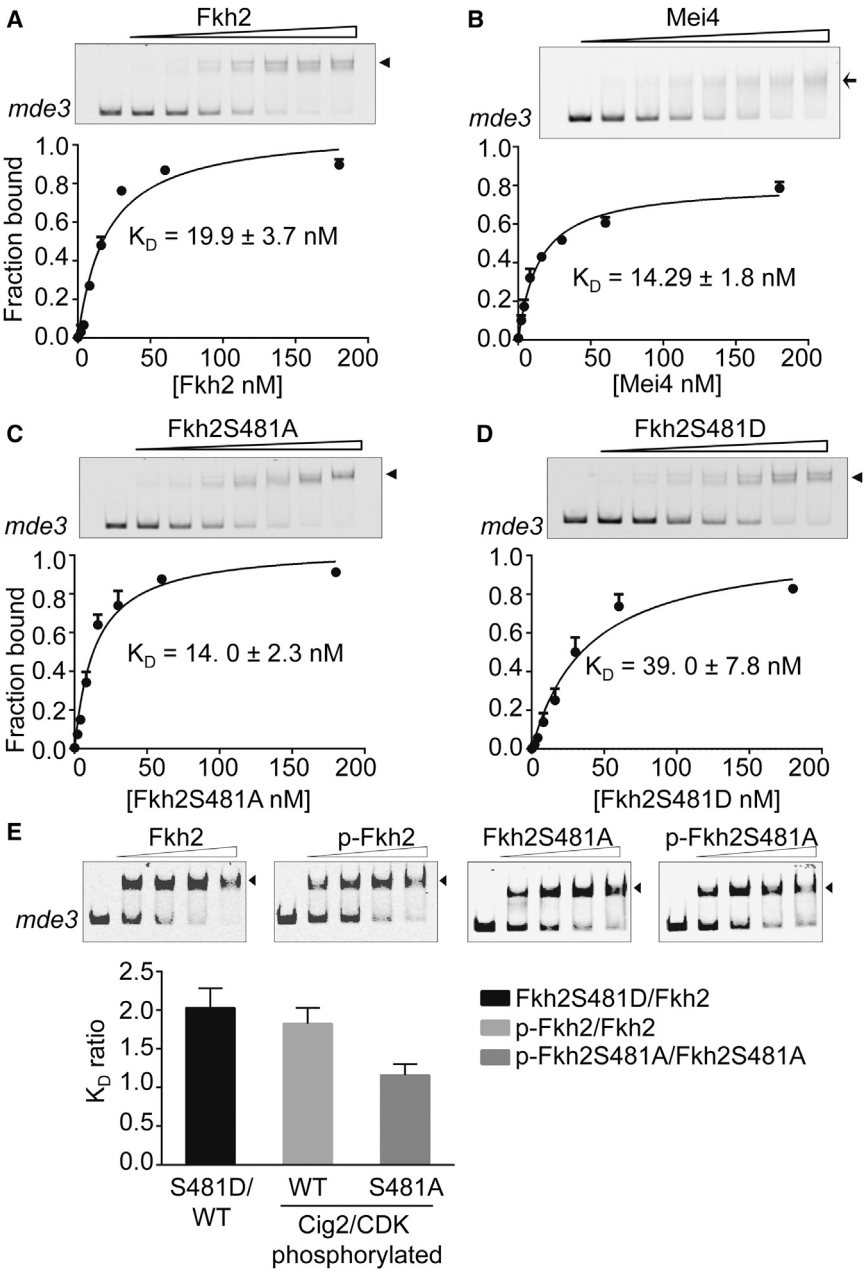

Figure 4. Fkh2 Phosphorylation Decreases Its Affinity for Promoter Binding In Vitro

(A) Electrophoretic mobility shift assay (EMSA) using purified Fkh2 and the 5′ end-labeled promoter region of *mde3*. Increasing concentrations of purified Fkh2 (2, 4, 8, 16, 30, 60, and 180 nM) were used to calculate the K_D. The quantity of bound DNA was represented as the function of the total concentration of the DNA in the assays. K_D values were estimated by fitting the binding curve using Prism 5 GraphPad software. Arrowhead indicates the Fkh2/*mde3* complex.

(B) EMSA using different concentrations of purified His-Mei4 (2, 4, 8, 16, 30, 60, and 180 nM). The quantity of bound DNA is represented as the function of the total concentration of the DNA in the assays. K_D values were estimated as in (A). Arrow indicates the Mei4/*mde3* complex.

(C) Same as in (A) but using increasing concentrations of Fkh2S481A (2, 4, 8, 16, 30, 60, and 180 nM). Arrowhead indicates the Fkh2 S481A/*mde3* complex.

(D) Same as in (A) but using increasing concentrations of Fkh2 S481D (2, 4, 8, 16, 30, 60, and 180 nM). Arrowhead indicates the Fkh2 S481D/*mde3* complex.

(E) EMSAs using Fkh2 or Fkh2S481A phosphorylated in vitro. Fkh2 and Fkh2S481A proteins were used as substrates in a kinase assay in the absence (FKh2 or Fkh2S481A) or presence of Cig2/CDK (p-Fkh2 or p-Fkh2S481A, respectively). After the phosphorylation assay, increasing concentrations of each protein were used for the EMSA with the promoter region of *mde3*. Arrowhead indicates the Fkh2/*mde3* complex. The K_D ratio of Fkh2S481D versus Fkh2 or in vitro phosphorylated versus unphosphorylated proteins is represented in the bottom graphic.

In all five panels, error bars (SEM) were calculated from at least three experiments.

See also Figure S3.

substrates for Cig2/Cdk1 in vitro phosphorylation assays. After treatment with the kinase, the resulting protein was used in our EMSAs to determine their affinity for DNA, comparing wild-type with S481A and the different effect of the phosphorylation. As shown in Figure 4E, while wild-type Fkh2 decreases its affinity for DNA when it is phosphorylated by Cig2/Cdk1, we could not appreciate any effect when using the S481A mutant. In fact, the decrease in affinity observed on wild-type Fkh2 when was phosphorylated was very similar to the decrease in affinity when the S481D was compared to the wild-type Fkh2. We conclude that the phosphorylation of Fkh2 at serine 481 by Cig2/Cdk1 is responsible for the observed decrease of affinity to *mde3* promoter.

Fkh2 and Mei4 Do Not Bind Simultaneously to DNA

To test whether phosphorylation of Fkh2 might affect its binding in the presence of Mei4, we decided to do competition assays using a constant protein concentration of Mei4 and increasing amounts of Fkh2 (Figure S4). To our surprise, we could not detect binding of both transcription factors to the same probe, that is, we could not detect a supershift containing both Mei4 and Fkh2. On the contrary, when using Fkh2 concentrations below the K_D we could only detect the complex between the probe and Mei4. When we increased Fkh2 concentrations, Fkh2 displaced Mei4 from the complex, but when the phosphomimetic mutant was used (Fkh2S481D), higher concentrations of Fkh2 were required to completely displace Mei4 from the probe. This result let us to hypothesize that, contrary to what we expected, Fkh2 might not be loading Mei4 into the meiotic genes but instead might be competing with Mei4 for binding to these genes until Cig2/CDK

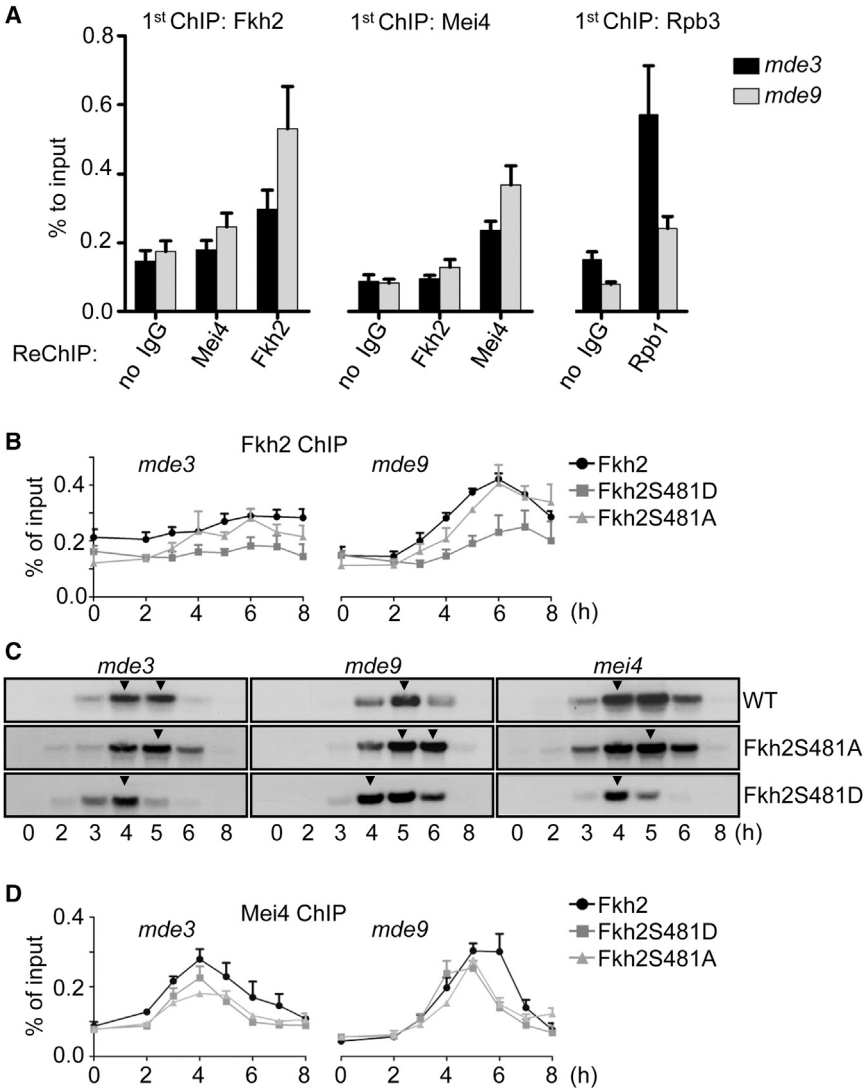

Figure 5. Fkh2 and Mei4 Bind DNA in a Mutually Exclusive Manner

(A) Left: α-HA (Fkh2) immunoprecipitated chromatin from meiotic (5 hr) extracts prepared from a Fkh2-HA Mei4-Myc strain were used to re-ChIP with either no antibody (no immunoglobulin G [IgG]) or α-Myc (for Mei4) or α-HA (for Fkh2) antibodies. Middle: same as in the left panel, using the reverse-tagged strain, Mei4-HA Fkh2-Myc, allowed to ChIP Mei4 (α-HA) and re-ChIP with either no antibody (no IgG) or α-Myc (for Fkh2) or α-HA (for Mei4) antibodies. Right: chromatin isolated from a Rbp3-HA Rbp1-Myc strain was immunoprecipitated with α-HA antibodies and subjected to a second round of immunoprecipitation with no IgG or α-Myc antibodies. In all three panels, average values ± SEM from at least three experiments were plotted. The enrichment values are expressed as percentage of the input.

(B) Fkh2 ChIP analysis during synchronous meiosis in WT (Fkh2), hypophosphorylated Fkh2 (Fkh2S481A), and phosphomimetic Fkh2 (Fkh2S481D) cells. Chromatin was immunoprecipitated with α-HA antibody, and the isolated DNA was used to amplify the promoter region of *mde3* and *mde9*. Plots represent the average of at least three different biological replicates ± SEM.

(C) Northern blot analysis of wild-type (WT) and Fkh2 phosphorylation mutants (Fkh2S418A and Fkh2S418D) strains. RNA isolated from synchronous meiosis was resolved (10 μg) and hybridized with the probes indicated on top. Arrowheads indicate the time of meiosis in which the maximum expression is achieved.

(D) Mei4 ChIP analysis during synchronous meiosis in WT (Fkh2), hypophosphorylated Fkh2 (Fkh2S481A), and phosphomimetic Fkh2 (Fkh2S481D) cells. Chromatin was immunoprecipitated with α-HA antibody, and the isolated DNA was used to amplify the promoter region of mde3 and mde9. Plots represent the average of at least three independent experiments ± SEM.

See also Figures S4 and S5.

phosphorylates Fkh2. Thus, Fkh2 would mark some specific promoters inducing the later binding of Mei4.

Many transcription factors bind DNA as dimers (hetero- or homodimers); alternatively, they may bind to proximal sites in the same promoter. To determine if Mei4 might directly interact with Fkh2, we decided to carry out coprecipitations using specific antibodies. We were able to detect a reciprocal in vitro interaction between both proteins in the soluble fraction of formaldehyde-crosslinked extracts (data not shown). To determine whether this interaction occurred when these proteins were bound to DNA in an overlapping manner or whether they bound DNA in a mutually exclusive manner (as deduced from our in vitro EMSA experiments; Figure S4), we performed ChIP-re-ChIP experiments (Figure 5A). As expected, Fkh2 was detected at the *mde3* promoter and at the *mde9* promoter; however, we were unable to detect Mei4 in these promoters from meiotic extracts that were previously immunoprecipitated by Fkh2. The reverse experiment showed that we could detect Mei4 in their target promoters, but we could not detect Fkh2 in these immunoprecipitates. Since ChIP-re-ChIP experiments are quite challenging experiments in which the difference between a positive result and a negative one is minimal, we decided to use two constitutive subunits of RNA polymerase II, Rbp1 and Rbp3, as a control for our experiments. As shown in the right panel, and using the same setting, we were able to detect re-ChIP between the two subunits of RNA polymerase II on the same promoters. These results indicate that Fkh2 and Mei4 (although they can coimmunoprecipitate in soluble extracts) do not temporarily co-occupy the same target promoters: Fkh2 and Mei4 interaction cannot take place while binding to DNA. On the contrary, they point to the possibility that Fkh2 has to bind earlier than Mei4, helping to maintain an open chromatin structure depleted of nucleosomes, but also has to be released from DNA before Mei4 is loaded onto the same target promoters.

To fully characterize the molecular mechanism of Fkh2/Mei4-mediated transcription and to analyze the in vivo role of

Fkh2Ser481 phosphorylation, we replaced the endogenous Fkh2 by mutated versions in which Ser481 was changed to alanine (Fkh2S481A) or aspartic acid (Fkh2S481D) to constitutively mimic the hypophosphorylated and hyperphosphorylated forms of Fkh2 at Ser481. Both strains displayed growth rate, shape, and viability similar to a wild-type strain during mitotic growth. However, when induced to enter into meiosis, they had a lower spore viability compared to the wild-type strain (Fkh2S481A: 72% ± 3%; Fkh2S481D: 75% ± 5%; wild-type: 94% ± 5%). We induced synchronous meiosis in both strains and analyzed the Fkh2-binding profile along meiosis compared to a wild-type strain (Figure 5B). While the hypophosphorylated mutant (Fkh2S481A) has a similar binding profile to the wild-type Fkh2, the phosphomimetic mutant (Fkh2S481D) binds with weaker affinity both to the *mde3* promoter and, especially, to the *mde9* promoter. In parallel, we analyzed the transcription profile of both strains compared to a wild-type strain (Figures 5C and S5). The Fkh2S481A strain, which maintains Fkh2 with higher affinity to the FLEX elements in vitro (Figure 4) and in vivo (Figure 5B), delays the onset of the meiotic transcription program for ~1 hr. On the contrary, we could observe an advancement of the meiotic transcription program in the Fkh2S481D strain, which has less affinity for promoters than Mei4 and, consequently, can be easily displaced from chromatin by lower Mei4 concentrations. As expected, Mei4 binds prematurely when cells expressed the phophomimetic Fkh2 (Figure 5D), with an effect that was more noticeable for *mde9* than for *mde3* promoters (similarly to what we observed for Fkh2 binding and for *mde9* expression, as shown in Figures 5B and 5C).

DISCUSSION

In the past few years, several studies have shed light of the pivotal role of the forkhead box (FOX) proteins in chromatin remodeling. Members of the FOXA subfamily have been shown to open up chromatin directly by interacting with specific DNA sequences within compact chromatin, promoting nucleosome decompactation, and thus increasing the binding of other transcription factors (Cirillo et al., 2002; Lalmansingh et al., 2012). FOXA1 serves as pioneer factor of estrogen receptor in breast cancer cells, where FOXA1 is constitutively bound to chromatin regions that are also bound by ER following estrogen treatment. When FOXA1 is knockdown by RNAi, there is a decrease in ER binding, decreased cofactor recruitment and decreased estrogen-stimulation (Zaret and Carroll, 2011). The FOXO subfamily is placed in a unique class of proteins that act as pioneer factors as well as classic transcription factors. FOXO proteins can interact with core histones disrupting histone-DNA interactions (Lalmansingh et al., 2012). FOXO is proposed to bind to closed chromatin, recruiting chromatin-remodeling complexes, or it can open compacted nucleosomes in vitro in the absence of an ATP-dependent chromatin remodeler such as SWI/SNF. The two mechanisms need not be mutually exclusive, since FOXO can first bind to and open regions of highly compacted chromatin and subsequently recruit chromatin remodelers to extend or maintain the open conformation (Zaret and Carroll, 2011).

Fission yeast has four genes that code for proteins containing forkhead domains: *fkh2*, *sep1*, *mei4* and *fhl1* (Buck et al., 2004; Horie et al., 1998; Szilagyi et al., 2005). Very little is known regarding Fhl1, and no target genes of this transcription factor have yet been characterized. Fkh2 and Sep1 have been shown to work together and are essential to control periodic gene transcription during the mitotic cell cycle, being responsible for the M-to-G1 transcriptional wave (Papadopoulou et al., 2008). In fact, it has been suggested that Fkh2 and Sep1 have respective negative and positive roles in regulating transcription during mitotic growth (Rustici et al., 2004). Furthermore, it has also been proposed that Fkh2 represses the expression of Mei4 targets during vegetative growth (Chen et al., 2012). During meiosis, it was suggested that a meiotic-specific forkhead, Mei4, would replace Sep1 to work together with Fkh2, keeping the positive and negative roles in transcription regulation although controlling the transcription and splicing of a set of meiotic-specific genes (Moldón et al., 2008). Recent studies have shown that *S. pombe*, Fkh2 co-precipitates with Nts1, a component of the Clr6 HDAC complex (Zilio et al., 2014), which supports the idea of the involvement of Fkh2 in the repression of transcription. Similarly, budding yeast Fkh2 recruits the HDAC Rpd3(L) to the CTS1 promoter (Voth et al., 2007).

Here, we show that the binding of Fkh2 to the promoter of meiotic genes (during mitotic growth and during early meiosis) works mainly as a repressor. However, Fkh2 is more than a simple repressor: in fact, we propose that Fkh2 could be a bona fide pioneer factor that acts as landing pad for the later binding of the activating transcription factor Mei4 (Figure 6). The binding of Fkh2 before Mei4 helps to establish an NDR, which in turn can phase other local binding sites on or off of nucleosomes to allow Mei4 binding. This implies that Fkh2 creates a timely window of opportunity to induce the transcription of the Mei4-dependent genes. Thus, Fkh2 has two faces, since during mitotic growth and early meiosis, it is involved in the repression of transcription, and it is required for the later binding of Mei4 and the consequent transcription activation of the Mei4-dependent genes. In fact, in the absence of Fkh2, the meiotic gene expression program is hampered and delayed. This dual role of Fkh2 is achieved by direct competition between Fkh2 and Mei4 for binding to the same subset of promoters. Although they can form heterodimers in solution (data not shown), they do not co-exist bound to the same promoters (Figures 5A and S4). Thus, to induce transcription of the meiotic genes, Fkh2 has to be overturned by Mei4. This is achieved by two related mechanisms. First, Fkh2 is phosphorylated in a CDK-Cig2-dependent manner, decreasing its affinity for DNA. In fact, a genetic interaction between Cig2 and Mei4 has been previously described, which supports this observation (Malapeira et al., 2005). In addition, *mei4* transcription is autoregulated through a positive feedback loop (Abe and Shimoda, 2000), helping to accumulate enough Mei4 to push Fkh2 away from the target promoters. This equilibrium between Fkh2 (as a repressor) and Mei4 (as an activator) marks the time when the Mei4-dependent genes are transcribed during meiosis. It is important to point out that the affinity of Fkh2 for FLEX motifs cannot be dramatically impaired: most mitotic genes

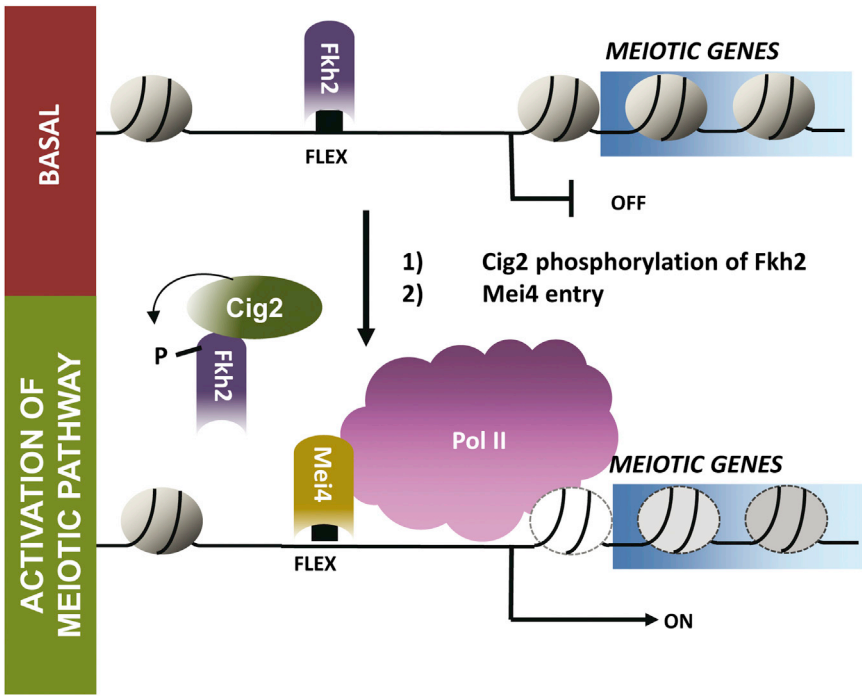

Figure 6. Model of the Coordinated Regulation of Fkh2 and Mei4 during Meiosis

During mitotic growth, Fkh2 constitutively binds to most Mei4-regulated meiotic genes. This binding helps to silence its expression. Once in meiosis, Cig2 phosphorylates Fkh2, decreasing its affinity toward the FLEX motifs. At the same time, Mei4 accumulates in the nucleus, displacing Fkh2 from the Mei4-target genes.

regulated by Fkh2 are essential for fitness and, thus, one could not expect an on/off response by CDK phosphorylation without compromising viability; however, we observe an advancement or delay of 1 hr (out of the 8 hr that takes to complete a meiosis in fission yeast) of the transcriptional program (Figures 5C and S5), compromising spore viability.

EXPERIMENTAL PROCEDURES

Strains and Media

All *S. pombe* strains used in this study are listed in Table S2. Media were prepared as described previously (Moreno et al., 1991). Cells were grown at 25°C for *pat1-114* or at 30°C for *pat1.L95G* in minimal media supplemented with leucine (100 μg/ml) when required. To induce meiosis, when cells reached mid-log phase, the culture was either shifted to 35.5°C, in the case of *pat1-114* (ChIP-seq experiments and to prepare extracts for the in vitro kinase assay shown in Figure 3), or the ATP analog 3-MB-PP1 was added to the pat1.L95G background cells (the rest of the experiments shown in this paper). Synchronicity was measured by DAPI staining as described previously (Guerra-Moreno et al., 2012). We did not start our meiotic experiments from G1-synchronized fission yeast cells, because when synchronized by nitrogen starvation, the quality of the ChIP experiments was extremely low, with a percentage of immunoprecipitated DNA values close to the limits of the background detection (perhaps a high protein degradation rate after nitrogen starvation might be the cause). On the contrary, when Mei4 and/or Fkh2 were chromatin immunoprecipitated from cells that had not been nitrogen starved, we could obtain reproducible ChIPs, with values that could be statistically trusted. Although it is essential to enter meiosis from G1 followed from pre-meiotic S phase to have reductional meiosis I (Watanabe et al., 2001), we strongly believe that it does not matter from the point of view of the mid-meiosis regulation of transcription (Mei4- and Fkh2-regulated gene expression program). The Mei4 expression profile is the same when meiosis is induced from G1 or from not-synchronized cultures (unpublished data). Furthermore, the meiotic transcriptional program is well preserved regardless of whether the cells enter meiosis from G1 or G2, with the exception of the genes that are expressed during the pre-meiotic S phase (Watanabe et al., 2001). Representative plots showing the synchronicity achieved is shown in Figure S6. To determine spore viability, we performed random spore analysis. Briefly, after mating the haploid parental cells, the cell-ascus mixture was treated with β-glucuronidase (Roche). Spore concentration in the suspension was determined, and 250 spores were spread on YE5S plates (in duplicate). After 2–3 days at 30°C, the number of colonies was counted.

Preparation of *S. pombe* TCA Extracts and Immunoblot Analysis

To analyze levels of Fkh2 and Mei4 proteins, trichloroacetic acid (TCA) extracts were prepared as previously described (Sansó et al., 2008). Immunoblot was performed using anti-hemagglutinin (ant-HA) (12CA5) or anti-Myc (9E10) monoclonal antibodies. Anti-Sty1 (Jara et al., 2007) was used as loading control.

Construction of Fkh2 Mutant Strains

To construct Fkh2 strains with serine 481 mutated, we performed site-directed mutagenesis on a plasmid containing the *fkh2* coding region amplified by PCR. These plasmids were then used as templates for PCR, and the resulting DNA fragments were introduced into *fkh2::ura4* cells by transformation. The mutations were confirmed by PCR and sequencing.

ChIP and ChIP Re-ChIP

ChIP and ChIP re-ChIP were performed essentially as described previously (Moldón et al., 2008). For ChIP re-ChIP, the first immunoprecipitation was performed using protein G- anti-HA-crosslinked beads. The eluates of three primary immunoprecipitations were combined, diluted ten times with lysis buffer without SDS, and subjected to the second immunoprecipitation. Results are shown as percentage of input, as described elsewhere (Sadasivam et al., 2012). All the experiments were plotted as the average of at least three replicates ± SEM.

Gene Expression Analysis

RNA extraction was performed as described previously (Moldón et al., 2008), and 10 μg total RNA was analyzed by northern blot. The *mde9, mde3*, and *mei4* probes contained a ^{32}P-labeled region of ~1 kb of each open reading frame (ORF).

Production of Recombinant Proteins

For production of glutathione S-transferase (GST)-Fkh2 chimeras used as substrates in the kinase assay, we cloned a full-length Fkh2 ORF in the pGEX-4T1 (GE Healthcare). The GST-Fkh2 Δ457–528 was constructed by *NdeI* and EcoRI partial digestion of this plasmid. To construct the Fkh2 phosphorylation mutants, a truncated version of Fkh2 (aa 457–528) was cloned into the pGEX-4T1 plasmid and used for site-directed mutagenesis of S462, S481, and S528 to alanine. To express GST-tagged versions of Fkh2 used in the EMSA assays, we cloned the full-length ORFs of Fkh2, Fkh2S481A, and Fkh2S481D in the multicloning site of vector pGEX-2T-TEV (that encode the GST tag followed

by a TEV protease cleavage site). All the GST-Fkh2 chimeras used in this study were expressed in the FB810 *E .coli* strain and purified following GE Healthcare instructions. The His-Mei4 protein was expressed using the pRSET-A plasmid (Invitrogen) in the BL21DE3 strain and purified by His-Trap HP columns and an FPLC system (GE Healthcare) following the manufacturer's instructions.

Electrophoretic Mobility Shift Assay

We performed the EMSA using as a probe either a 112-bp region of the *mde3* promoter (that included one FLEX sequence) or a 148-bp region of the *mde9* promoter (with three FLEX sequences); probes were labeled with the infrared dye DY-682 (LI-COR) by PCR amplification. *E. coli* purified proteins were incubated for 30 min at 4°C with 1 fmol labeled DNA probe in a total volume of 10 μl containing 10 mM Tris-HCL (pH 8), 40 mM KCL, 6% glycerol, 2.5 mM DTT, 0.25% Tween 20, and poly(dI-dC) (0.02 mg/ml). DNA-protein complexes were resolved by nondenaturing electrophoresis on a 6% polyacrylamide gel (29 acrilamide:1 bisacrilamide), 1% glycerol, in 1× TAE buffer. The gels were visualized using a LI-COR Odyssey imaging system. To calculate the endogenous protein concentration of Fkh2 and Mei4, and since there is no published information regarding Mei4 protein concentration, we did a western blot to compare the amount of Fkh2 and Mei4 in meiosis (interval of 3–5 hr) to the published amount of Fkh2 in vegetative cells (Carpy et al., 2014); we used a strain in which endogenous Fkh2 and Mei4 were tagged with 3× HA, and by correlation, we calculated the concentrations of both Fkh2 and Mei4 during meiosis (Figure S7).

Kinase Assays

For the in vitro kinase assay, protein extracts (50 μg) from cells expressing HA-tagged Cig2 were immunoprecipitated with anti-HA monoclonal antibody. Immunoprecipitates were washed in NET-N buffer (20 mM Tris [pH 8.0], 100 mM NaCl, 1 mM EDTA, 0.5% NP-40, 1 mM DTT, 0.5 mM PMSF, 5 μg/ml leupeptin, and 5 μg/ml aprotinin) followed by kinase buffer (100 mM HEPES [pH 7.5], 20 mM $MgCl_2$, 4 mM EGTA, and 2 mM DTT) and incubated with histone H1 (1 μg) and 10 μCi of [γ-^{32}P]ATP or with purified Fkh2 (300 ng). After 20 min at 30°C, the reactions were stopped with sample buffer, and the proteins were separated by 11% SDS-PAGE and detected by autoradiography. When used on EMSA, reactions were cooled on ice, spun down, and the substrate (Fkh2) used directly on EMSA.

ACCESSION NUMBERS

The accession number for the data reported in this paper is European Nucleotide Archive (ENA): ERP001894.

SUPPLEMENTAL INFORMATION

Supplemental Information includes Supplemental Experimental Procedures, seven figures, and three tables and can be found with this article online at http://dx.doi.org/10.1016/j.celrep.2015.12.074.

AUTHOR CONTRIBUTIONS

I.A.-R., A.M., and A.P.V. conducted the experiments; I.A.-R., E.H., and J.A. designed the experiments; I.A.-R., P.G.F., E.H., R.G., and J.A. analyzed and interpret the data; and I.A.-R., P.G.F., A.M., E.H., and J.A. wrote the manuscript.

ACKNOWLEDGMENTS

We thank Sergio Moreno, Chris McInerny, and Damien Hermand for strains. We thank Charles Query for critical reading of the manuscript and members of the Oxidative Stress and Cell Cycle laboratory for helpful discussions and many inputs. We acknowledge the technical support of Mercè Carmona. We thank Angad Garg, Bruce Futcher, and Janet Leatherwood for sharing results before publication. This work was supported by grants from the Spanish Ministerio de Economia y Competitividad (MINECO) (grants BFU2012-31939 and BFU2015-66347), PLAN E, and Feder. E.H. is a recipient of an ICREA Academia Award (Generalitat de Catalunya).

Received: September 14, 2015
Revised: November 13, 2015
Accepted: December 15, 2015
Published: January 21, 2016

REFERENCES

Abe, H., and Shimoda, C. (2000). Autoregulated expression of Schizosaccharomyces pombe meiosis-specific transcription factor Mei4 and a genome-wide search for its target genes. Genetics *154*, 1497–1508.

Borgne, A., Murakami, H., Ayté, J., and Nurse, P. (2002). The G1/S cyclin Cig2p during meiosis in fission yeast. Mol. Biol. Cell *13*, 2080–2090.

Buck, V., Ng, S.S., Ruiz-Garcia, A.B., Papadopoulou, K., Bhatti, S., Samuel, J.M., Anderson, M., Millar, J.B., and McInerny, C.J. (2004). Fkh2p and Sep1p regulate mitotic gene transcription in fission yeast. J. Cell Sci. *117*, 5623–5632.

Bulmer, R., Pic-Taylor, A., Whitehall, S.K., Martin, K.A., Millar, J.B., Quinn, J., and Morgan, B.A. (2004). The forkhead transcription factor Fkh2 regulates the cell division cycle of Schizosaccharomyces pombe. Eukaryot. Cell *3*, 944–954.

Carpy, A., Krug, K., Graf, S., Koch, A., Popic, S., Hauf, S., and Macek, B. (2014). Absolute proteome and phosphoproteome dynamics during the cell cycle of Schizosaccharomyces pombe (fission yeast). Mol. Cell. Proteomics *13*, 1925–1936.

Chen, H.M., Rosebrock, A.P., Khan, S.R., Futcher, B., and Leatherwood, J.K. (2012). Repression of meiotic genes by antisense transcription and by Fkh2 transcription factor in Schizosaccharomyces pombe. PLoS ONE *7*, e29917.

Cipak, L., Hyppa, R.W., Smith, G.R., and Gregan, J. (2012). ATP analog-sensitive Pat1 protein kinase for synchronous fission yeast meiosis at physiological temperature. Cell Cycle *11*, 1626–1633.

Cirillo, L.A., Lin, F.R., Cuesta, I., Friedman, D., Jarnik, M., and Zaret, K.S. (2002). Opening of compacted chromatin by early developmental transcription factors HNF3 (FoxA) and GATA-4. Mol. Cell *9*, 279–289.

Darieva, Z., Clancy, A., Bulmer, R., Williams, E., Pic-Taylor, A., Morgan, B.A., and Sharrocks, A.D. (2010). A competitive transcription factor binding mechanism determines the timing of late cell cycle-dependent gene expression. Mol. Cell *38*, 29–40.

Guerra-Moreno, A., Alves-Rodrigues, I., Hidalgo, E., and Ayté, J. (2012). Chemical genetic induction of meiosis in *Schizosaccharomyces pombe*. Cell Cycle *11*, 1621–1625.

Harigaya, Y., and Yamamoto, M. (2007). Molecular mechanisms underlying the mitosis-meiosis decision. Chromosome Res. *15*, 523–537.

Harigaya, Y., Tanaka, H., Yamanaka, S., Tanaka, K., Watanabe, Y., Tsutsumi, C., Chikashige, Y., Hiraoka, Y., Yamashita, A., and Yamamoto, M. (2006). Selective elimination of messenger RNA prevents an incidence of untimely meiosis. Nature *442*, 45–50.

Horie, S., Watanabe, Y., Tanaka, K., Nishiwaki, S., Fujioka, H., Abe, H., Yamamoto, M., and Shimoda, C. (1998). The Schizosaccharomyces pombe mei4+ gene encodes a meiosis-specific transcription factor containing a forkhead DNA-binding domain. Mol. Cell. Biol. *18*, 2118–2129.

Jara, M., Vivancos, A.P., Calvo, I.A., Moldón, A., Sansó, M., and Hidalgo, E. (2007). The peroxiredoxin Tpx1 is essential as a H2O2 scavenger during aerobic growth in fission yeast. Mol. Biol. Cell *18*, 2288–2295.

Lalmansingh, A.S., Karmakar, S., Jin, Y., and Nagaich, A.K. (2012). Multiple modes of chromatin remodeling by Forkhead box proteins. Biochim. Biophys. Acta *1819*, 707–715.

Lee, C.S., Friedman, J.R., Fulmer, J.T., and Kaestner, K.H. (2005). The initiation of liver development is dependent on Foxa transcription factors. Nature *435*, 944–947.

Lino, Y., and Yamamoto, M. (1985). Mutants of Schizosaccharomyces pombe which sporulate in the haploid state. Mol. Gen. Genet. *198*, 416–421.

Malapeira, J., Moldón, A., Hidalgo, E., Smith, G.R., Nurse, P., and Ayté, J. (2005). A meiosis-specific cyclin regulated by splicing is required for proper progression through meiosis. Mol. Cell. Biol. *25*, 6330–6337.

Mata, J., Lyne, R., Burns, G., and Bähler, J. (2002). The transcriptional program of meiosis and sporulation in fission yeast. Nat. Genet. *32*, 143–147.

Mata, J., Wilbrey, A., and Bähler, J. (2007). Transcriptional regulatory network for sexual differentiation in fission yeast. Genome Biol. *8*, R217.

McLeod, M., and Beach, D. (1986). Homology between the *ran1+* gene of fission yeast and protein kinases. EMBO J. *5*, 3665–3671.

McLeod, M., and Beach, D. (1988). A specific inhibitor of the *ran1+* protein kinase regulates entry into meiosis in *Schizosaccharomyces pombe*. Nature *332*, 509–514.

Moldón, A., Malapeira, J., Gabrielli, N., Gogol, M., Gómez-Escoda, B., Ivanova, T., Seidel, C., and Ayté, J. (2008). Promoter-driven splicing regulation in fission yeast. Nature *455*, 997–1000.

Moreno, S., Klar, A., and Nurse, P. (1991). Molecular genetic analysis of fission yeast Schizosaccharomyces pombe. Methods Enzymol. *194*, 795–823.

Papadopoulou, K., Ng, S.S., Ohkura, H., Geymonat, M., Sedgwick, S.G., and McInerny, C.J. (2008). Regulation of gene expression during M-G1-phase in fission yeast through Plo1p and forkhead transcription factors. J. Cell Sci. *121*, 38–47.

Rustici, G., Mata, J., Kivinen, K., Lió, P., Penkett, C.J., Burns, G., Hayles, J., Brazma, A., Nurse, P., and Bähler, J. (2004). Periodic gene expression program of the fission yeast cell cycle. Nat. Genet. *36*, 809–817.

Sadasivam, S., Duan, S., and DeCaprio, J.A. (2012). The MuvB complex sequentially recruits B-Myb and FoxM1 to promote mitotic gene expression. Genes Dev. *26*, 474–489.

Sansó, M., Gogol, M., Ayté, J., Seidel, C., and Hidalgo, E. (2008). Transcription factors Pcr1 and Atf1 have distinct roles in stress- and Sty1-dependent gene regulation. Eukaryot. Cell *7*, 826–835.

Shimada, M., Yamada-Namikawa, C., Murakami-Tonami, Y., Yoshida, T., Nakanishi, M., Urano, T., and Murakami, H. (2008). Cdc2p controls the forkhead transcription factor Fkh2p by phosphorylation during sexual differentiation in fission yeast. EMBO J. *27*, 132–142.

Soriano, I., Quintales, L., and Antequera, F. (2013). Clustered regulatory elements at nucleosome-depleted regions punctuate a constant nucleosomal landscape in Schizosaccharomyces pombe. BMC Genomics *14*, 813.

Szilagyi, Z., Batta, G., Enczi, K., and Sipiczki, M. (2005). Characterisation of two novel fork-head gene homologues of Schizosaccharomyces pombe: their involvement in cell cycle and sexual differentiation. Gene *348*, 101–109.

Voss, T.C., and Hager, G.L. (2014). Dynamic regulation of transcriptional states by chromatin and transcription factors. Nat. Rev. Genet. *15*, 69–81.

Voth, W.P., Yu, Y., Takahata, S., Kretschmann, K.L., Lieb, J.D., Parker, R.L., Milash, B., and Stillman, D.J. (2007). Forkhead proteins control the outcome of transcription factor binding by antiactivation. EMBO J. *26*, 4324–4334.

Watanabe, Y., and Yamamoto, M. (1994). S. pombe mei2+ encodes an RNA-binding protein essential for premeiotic DNA synthesis and meiosis I, which cooperates with a novel RNA species meiRNA. Cell *78*, 487–498.

Watanabe, Y., Shinozaki-Yabana, S., Chikashige, Y., Hiraoka, Y., and Yamamoto, M. (1997). Phosphorylation of RNA-binding protein controls cell cycle switch from mitotic to meiotic in fission yeast. Nature *386*, 187–190.

Watanabe, Y., Yokobayashi, S., Yamamoto, M., and Nurse, P. (2001). Premeiotic S phase is linked to reductional chromosome segregation and recombination. Nature *409*, 359–363.

Xu, J., Watts, J.A., Pope, S.D., Gadue, P., Kamps, M., Plath, K., Zaret, K.S., and Smale, S.T. (2009). Transcriptional competence and the active marking of tissue-specific enhancers by defined transcription factors in embryonic and induced pluripotent stem cells. Genes Dev. *23*, 2824–2838.

Yamashita, A., Shichino, Y., Tanaka, H., Hiriart, E., Touat-Todeschini, L., Vavasseur, A., Ding, D.Q., Hiraoka, Y., Verdel, A., and Yamamoto, M. (2012). Hexanucleotide motifs mediate recruitment of the RNA elimination machinery to silent meiotic genes. Open Biol. *2*, 120014.

Zaret, K.S., and Carroll, J.S. (2011). Pioneer transcription factors: establishing competence for gene expression. Genes Dev. *25*, 2227–2241.

Zilio, N., Codlin, S., Vashisht, A.A., Bitton, D.A., Head, S.R., Wohlschlegel, J.A., Bähler, J., and Boddy, M.N. (2014). A novel histone deacetylase complex in the control of transcription and genome stability. Mol. Cell. Biol. *34*, 3500–3514.